

Supporting Information

Adverse to Beneficial: Upcycling Residual Lithium Compounds on $\text{LiNi}_{0.8}\text{Mn}_{0.1}\text{Co}_{0.1}\text{O}_2$ into stabilizing $\text{Li}_{1+x}\text{Mn}_{2-x}\text{O}_4$ Interface

Jyotirekha Dutta^{1,2}, Shuvajit Ghosh¹, Vilas G. Pol², Surendra K. Martha^{1, *}

¹*Department of Chemistry, Indian Institute of Technology Hyderabad, Kandi, Sangareddy, 502284, Telangana, India.*

²*Davidson School of Chemical Engineering, Purdue University, West Lafayette, IN 47907, USA.*

*Corresponding author.

Email address: martha@chy.iith.ac.in

1. Experimental section

1.1. Physical characterization

An Empyrean X'Pert Malvern Panalytical diffractometer (Cu K α radiation, 40 mA, 40 kV, $\lambda = 1.5406 \text{ \AA}$, $2\theta = 10^\circ\text{-}70^\circ$, scan rate 1° min^{-1}) was used to collect the powder X-ray diffraction (PXRD) patterns. A monochromatic Al K α (1486.6 eV) X-ray beam (20 mA, 15 kV) (performed on ESCA+ (Kratos, AXIS Nova, Shimadzu, Japan)) was used to analyze the X-ray photoelectron spectroscopy (XPS). The binding energies (BE) of all the elements were calibrated with respect to carbon BE (284.6 eV). The attenuated total reflection-infrared (ATR-IR) spectra were recorded using a Bruker Tensor 37 spectrophotometer. The Electron Paramagnetic Resonance (EPR) spectroscopy analysis was carried out by using a JEOL – JES-FA200 ESR spectrometer. The surface morphological analysis of PNMC and LMONMC was

carried out by using a field emission scanning electron microscope (FESEM, JEOL JEM 2011). A high-resolution transmission electron microscope (JEOL-JEM F200 TEM, Japan) was used to analyze the thickness and crystallinity of the surface layer. The scanning transmission electron microscopy–energy dispersive X-ray (STEM-EDX) mapping for all the elements was collected by using (STEM–EDX, JEOL JEM F200 TEM) mode. The pH of PNMC and LMONMC were measured by using a Systronics μ pH system 361 (India). For pH measurement, the samples were prepared by dispersing 3 g of each PNMC and LMONMC material in DI water in two separate beakers and stirred for 0.5 hours, followed by filtration. The filtrates were used for the pH measurements.

1.2. Electrode preparation, cell assembly, and electrochemical measurement

The slurries were made by taking an 8:1:1 ratio of active material (PNMC or LMONMC): additive (Super P carbon black): binder (poly (vinylidene fluoride) (PVDF), Kureha 1700, Japan in N-methyl pyrrolidone (Sigma-Aldrich) solvent, followed by casting onto an Al foil current collector (25 μ m thickness) by using a doctor blade technique and drying at 90 $^{\circ}$ C for 24 hours under vacuum. After the hot Calendering, the foils were punched into 10 mm discs. The active mass loading for all the electrodes was maintained at 5 ± 0.5 mg cm^{-2} .

The electrochemical performance studies were carried out by fabricating CR2032-type coin cells. The cells were fabricated inside an argon-filled glovebox (mBraun, Germany, H_2O and O_2 level < 0.1 ppm) using PNMC/LMONMC electrodes as a cathode, Li-chip as a counter and reference electrode, a polyethylene (PE) polypropylene (PP) trilayer separator (Celgard 2325, 39% porosity, 25 μ m), and 50 μ L of the electrolyte (1 m LiPF_6 salt in a 1:1 ratio of ethylene carbonate/ diethyl carbonate solvent). The cells were kept at rest for 24 hours after the fabrication and before conducting the electrochemical analysis.

Galvanostatic charge-discharge (GCD) analysis was carried out using an electrochemical analyzer (Biologic BCS805, France). The theoretical capacity of NMC811 was taken as 180 mAh g⁻¹ to calculate the current densities, and a voltage window of 3.0 – 4.3, 3.0 – 4.5, 3.0 – 4.7 V vs. Li⁺/Li was applied. For Chromolometry measurements, the working electrodes were polarized to 4.7 V vs. Li⁺/Li, and the current was measured by holding it at 4.7 V for 1.5 hours. The electrochemical impedance spectroscopy (EIS) measurement was done in the frequency range of 10⁵–10⁻² Hz at a voltage perturbation of 10 mV. All the electrochemical data presented here are the average electrochemical testing of 4–5-coin cells, with a ± 2% error range.

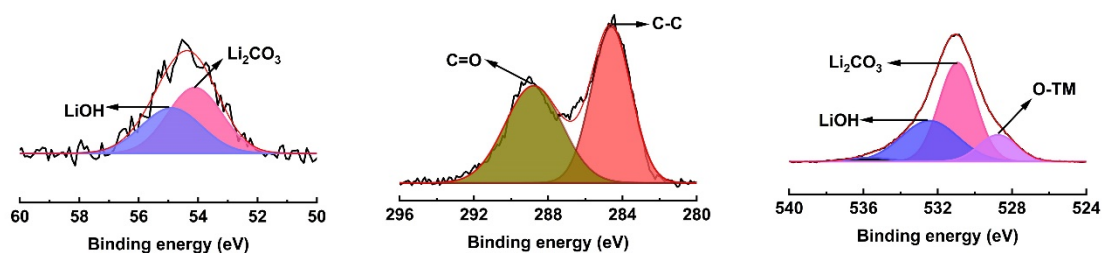


Figure S1: XPS spectra of PNMC (Li 1s, C 1s, O 1s) to support the presence of RLCs.

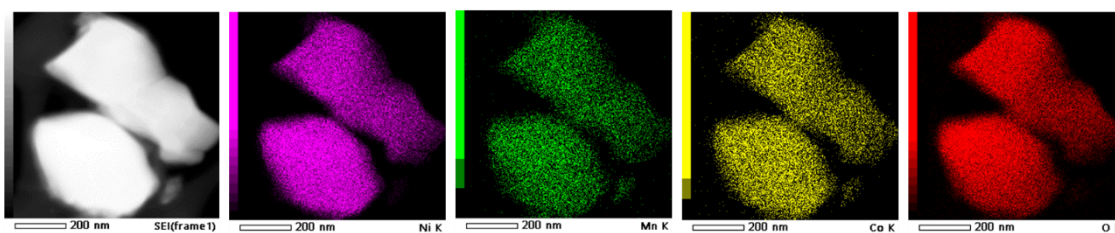


Figure S2: STEM-EDX elemental mapping of all the elements in PNMC.

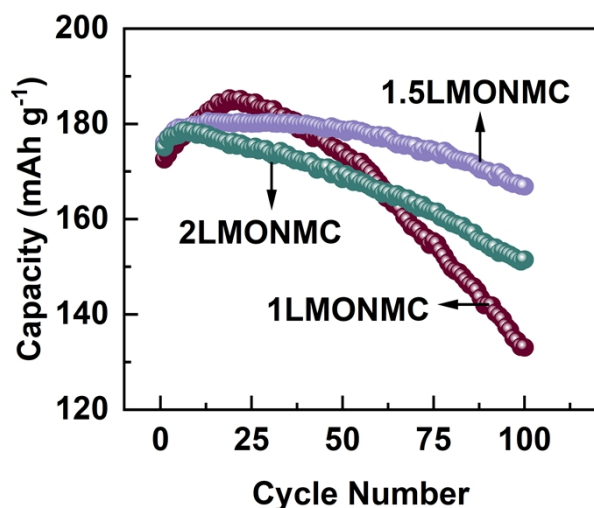


Figure S3: Comparison of cycle number vs. capacity at different (1 wt.%, 1.5 wt. %, and 2 wt. %) weight ratios to optimize the coating amount.

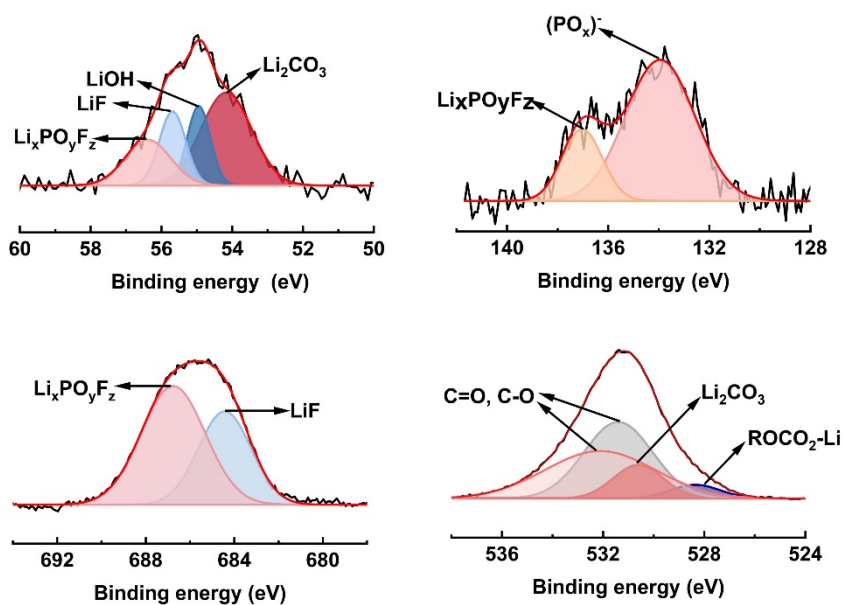


Figure S4: Post-cycling XPS (after 300th cycles at a current rate of 0.5 C, 3.0 – 4.3 V vs. Li⁺/Li) of PNMC (Li1s, P2p, F1s, O1s).

Table S1: The impedance parameters of PNMC and LPONMC in the 1st cycle and 300th cycle calculated from Figures 3h and 3i using the equivalent circuit model given in Fig. S5

NMC811	1 st cycle		300 th cycle	
	R ₁	R ₂	R ₁	R ₂
PNMC	5.7	30.0	22.9	100.5
LMONMC	5.4	20.9	16.9	48.0

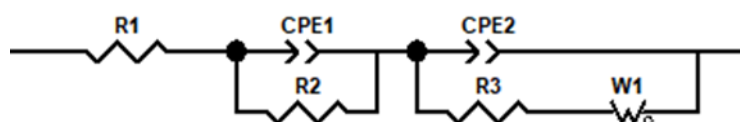


Figure S5: Equivalent circuit model to fit the experimental data. ‘R,’ ‘CPE,’ and ‘W’ refer to the resistance, constant phase element, and the Warburg impedance, respectively. R₁ is solution resistance. R₂ is a combination of interface crossing and charge transfer resistance.

Diffusion coefficient from EIS studies:

The Lithium-ion diffusion coefficient in PNMC and LMONMC is calculated from EIS studies (Figures 3h and 3i) by using the following formula:

$$D = \frac{0.5 R^2 T^2}{S^2 n^4 F^4 c^2 \sigma^2} \quad (1)$$

Where, D = Diffusion coefficient (cm² s⁻¹), R = universal gas constant (8.314 J K⁻¹ mol⁻¹), T = absolute temperature (in K), S = active surface area (in cm²), n = charge transfer number, F = Faraday’s constant (96485 C mol⁻¹), c = lithium-ion concentration (0.049 mol cm⁻³), σ = Warburg factor. The Warburg factor σ is correlated to Z’ (Ohm) by the following equation:

$$Z' = R_s + R_{ct} + \sigma \omega^{-1/2} \quad (2)$$

Z' is the real part, R_s = solution resistance, R_{ct} = charge transfer resistance, ω = angular frequency ($2\pi f$). Fig. 4 (d) and Fig. 4 (e) show the linear fitting of Z' (Ohm) vs. $\omega^{-1/2}$ plot. The slope of the plots is the Warburg factor (σ), which is used to calculate the diffusion coefficient (D).

Table S2: Diffusion coefficients of PNMCM and LMONMCM in the 1st cycle and 300th cycle.

NMC811	Diffusion coefficient (cm ² s ⁻¹)	
	At 1 st cycle	At the 300 th cycle
PNMCM	4.5 * 10 ⁻¹⁵	2.8 * 10 ⁻¹⁶
LMONMCM	2.1 * 10 ⁻¹⁴	1.0 * 10 ⁻¹⁵

Table S3: Comparison of our study with previously reported literature.

Coated interface	Electrochemical performances	Voltage window	Reference
LiF	50 %, 500 cycles	4.6 V	1
LiNbO ₃	88.8%, 200 cycles	2.8 – 4.3 V	2
LiMn _{1.9} Al _{0.1} O ₄	80%, 200 cycles	2.8 – 4.3 V	3
Li–Nb–O	89.6%, 60 cycles	3.0 – 4.5 V	4
Li_{1+x}Mn_{2-x}O₄	75 %, 300 cycles	3.0 – 4.3 V	This work
	84 %, 130 cycles	3.0 – 4.5 V	
	77 %, 100 cycles	3.0 – 4.7 V	

The advantages of our work compared to previous works are

1. Chemical conversion of adverse RLCs into a beneficial artificial interface comprising a chemically stable $\text{Li}_{1+x}\text{Mn}_{2-x}\text{O}_4$ interface via a single-step chemical reaction.
2. The formed interface significantly lowers the polarization for high-voltage $\text{H2} \rightarrow \text{H3}$ phase transition, thereby delaying the formation of microcracks.
3. The $\text{Li}_{1+x}\text{Mn}_{2-x}\text{O}_4$ interface enables high voltage (4.5 V and 4.7 V vs. Li^+/Li) stability of NMC811.

References:

- 1 J. Park, Y. Kim, Y. Kim, J. Park, D. G. Lee, Y. Lee, J. Hwang, K.-Y. Park and D. Lee, *Chemical Engineering Journal*, 2023, **467**, 143335.
- 2 G. Hu, Y. Tao, Y. Lu, J. Fan, L. Li, J. Xia, Y. Huang, Z. Zhang, H. Su and Y. Cao, *ChemElectroChem*, 2019, **6**, 4773–4780.
- 3 P. Oh, B. Song, W. Li and A. Manthiram, *Journal of Materials Chemistry A*, 2016, **4**, 5839–5841.
- 4 F. Xin, H. Zhou, X. Chen, M. Zuba, N. Chernova, G. Zhou and M. S. Whittingham, *ACS Appl. Mater. Interfaces*, 2019, **11**, 34889–34894.